Clays and Clay Minerals, Vol. 53, No. 4, 380–388, 2005.

THE HEAT CAPACITY OF THE SERPENTINE SUBGROUP MINERAL BERTHIERINE $(Fe_{2.5}Al_{0.5})[Si_{1.5}Al_{0.5}O_5](OH)_4$

CHRISTIAN BERTOLDI[1,*], EDGAR DACHS[1], LADO CEMIC[2], THOMAS THEYE[3], RICHARD WIRTH[4] AND WERNER GROGER[5]

[1]Abteilung Mineralogie und Materialwissenschaften, Fachbereich Geographie, Geologie und Mineralogie, Paris Lodron Universität Salzburg, Hellbrunnerstraße 34, 5020 Salzburg, Austria
[2]Institut für Geowissenschaften, Christian Albrechts Universität zu Kiel, Ludewig-Meyn-Strasse 10, 24118 Kiel, Germany
[3]Institut für Mineralogie und Kristallchemie, Universität Stuttgart, Azenbergstrasse 18, 70174 Stuttgart, Germany
[4]GeoForschungsZentrum Potsdam, Telegraphenberg, 14473 Potsdam, Germany
[5]Forschungsinstitut für Elektronenmikroskopie und Feinstrukturforschung, Technische Universität Graz, Steyrergasse 17, 8010 Graz, Austria

Abstract—The serpentine subgroup mineral berthierine was synthesized as a metastable precursor of the chlorite group mineral chamosite in cold seal pressure vessels at 575°C, 0.5 GPa and f_{O_2}-conditions of the NNO buffer from a glass of almandine bulk composition. The run products were investigated with X-ray powder diffraction (XRD), Mössbauer spectroscopy and electron microprobe analysis. One run product was also investigated by high-resolution transmission electron microscopy (HRTEM) and its heat capacity measured by heat pulse calorimetry and by differential scanning calorimetry in the temperature range 5–323 K. The XRD and HRTEM investigations clearly showed that the periodicity along the *c* axis of this sample is 7 Å demonstrating that the serpentine subgroup mineral berthierine of composition $(Fe^{2+}_{1.83}Fe^{3+}_{0.33}Al_{0.67})[Si_{1.33}Al_{0.67}O_5](OH)_4$ has formed in the synthesis experiments.

Integration of our heat capacity data, corrected to the composition $(Fe_{2.5}Al_{0.5})[Si_{1.5}Al_{0.5}O_5](OH)_4$ for end-member berthierine, yields a standard entropy of 284.1±0.3 J mol^{-1} K^{-1}. The C_p polynomial $C_p = 610.72 - 5140.0 \times T^{-0.5} - 5.8848 \times 10^6\ T^{-2} + 9.5444 \times 10^8\ T^{-3}$ is recommended for thermodynamic calculations above 298 K involving berthierine.

Key Words—Berthierine, Differential Scanning Calorimetry, Heat Capacity, Heat-pulse Calorimetry, Serpentine Subgroup Minerals, Standard Entropy.

INTRODUCTION

Berthierine is the preferred term for the trioctahedral Fe-dominant Al-substituted serpentine subgroup mineral with a periodicity of 7 Å along [001] (Bailey, 1988a). It occurs as fine-grained authigenic green clay in late Pleistocene to Holocene (<20 ka) shallow-marine sediments at depths not exceeding 80 m on continental shelves in tropical environments (verdine facies: Velde, 1985; Odin and Sen Gupta, 1988; Odin *et al.*, 1988; Ryan and Hillier, 2002). It is generated at or very near the sediment–sea interface due to chemical exchanges between sea water and sediment. Reported temperatures of formation for berthierine can be as low as 50°C (Velde, 1985). Iijima and Matsumoto (1982) demonstrated that berthierine in terrestrial coal measures is formed at the expense of kaolinite and siderite at low to medium diagenetic temperatures (65–130°C). Berthierine can also be found in low-grade metamorphic pelites (Mata *et al.*, 2001), diagenetic metasediments of volcanic origin (López-Munguira and Nieto, 2000; Schmidt *et al.*, 1999) as well as in laterites (Toth *et al.*, 1997).

It is well known from previous experiments aiming to synthesize clinochlore or chamosite that a serpentine subgroup mineral will form metastably prior to a chlorite group mineral (Yoder, 1952; Nelson and Roy, 1958; Gillery, 1959; Turnock, 1960; Hsu, 1968; James *et al.*, 1976; Cho and Fawcett, 1986). In nature, a precursor of berthierine is the mineral odinite (phyllite V) which is a poorly crystallized disordered di-trioctahedral Fe^{3+}-rich phyllosilicate with a periodicity along the *c* axis of 7 Å (Bailey, 1988b; Odin *et al.*, 1988), forming in shallow-marine environments of tropical regions at temperatures as low as 25°C (Porrenga, 1967). Odinite and berthierine transform to chamosite in diagenetic environments such as sedimentary ironstones and sandstones with grain-coating diagenetic chlorites in verdine facies environments (Kisch, 1983; Ahn and Peacor, 1985; Bailey, 1988b; Odin *et al.*, 1988; Odin, 1990; Walker and Thompson, 1990; Ehrenberg, 1993; Hillier, 1994; Hornibrook and Longstaffe, 1996; Ryan and Reynolds, 1996). Aagaard *et al.* (2000) provided experimental evidence that grain-coating chlorites form at the expense of berthierine at temperatures between 200 and 250°C and water pressures of 0.17 to 0.44 MPa.

There is some confusion concerning the nomenclature of serpentine and chlorite minerals: the terms "septe-

* E-mail address of corresponding author:
christian.bertoldi@sbg.ac.at
DOI: 10.1346/CCMN.2005.0530406

chlorite" and "7 Å-phase" (Nelson and Roy, 1958), "7 Å-structure" (Hsu, 1968), "7 Å-chlorite" (James *et al.*, 1976; Velde, 1985), "chlorite polymorph" (James *et al.*, 1976), "sedimentary 7 Å minerals", "berthierine" and "aluminous serpentine" (Velde, 1985) have been used for serpentine subgroup minerals. The terms "14 Å-structure" (Hsu, 1968), "14 Å-chlorite" (James *et al.*, 1976; Velde, 1985), "amesite" and "daphnite" (Holland and Powell, 1998) were applied to chlorite group minerals. In the older literature, the term chamosite was generally applied to minerals in ironstone deposits which frequently contain both Fe serpentine and Fe chlorite. Following Bailey (1980, 1988a), Deer *et al.* (1992) and Guggenheim *et al.* (1997) we propose to use "clinochlore" and "chamosite" for the Mg and Fe end-members of the chlorite group minerals, and "amesite" and "berthierine" for their analogues in the serpentine subgroup minerals.

For thermodynamic calculations and a better understanding of the phase relations of berthierine and chamosite, heat capacity is an important quantity. In this paper we report the first low-temperature heat capacity and differential scanning calorimetry (DSC) data for synthetic berthierine (5–323 K). We also present a C_p polynomial corrected to the end-member composition of berthierine $(Fe_{2.5}Al_{0.5})[Si_{1.5}Al_{0.5}O_5](OH)_4$, and the standard entropy derived from our heat capacity measurements.

EXPERIMENTAL METHODS

A glass of almandine bulk composition ($3FeO{\cdot}1Al_2O_3{\cdot}3SiO_2$) was produced by melting a stoichiometric mixture of ultra pure oxides (Fe_2O_3, Al_2O_3, SiO_2) at 1375ºC in a covered graphite crucible. The glass showed a greenish color due to the presence of Fe^{2+}. Under the microscope, no brownish patches were observed indicating the absence of Fe^{3+}. Berthierine was synthesized from this glass at 575ºC, 0.5 GPa in a hydrothermal apparatus under redox-conditions of the NNO buffer (details of the experimental method are given in Dachs, 1994). The run products were ground and examined by XRD (with a Siemens D-500 X-ray powder diffractometer with Ni-filtered CuKα radiation) and used as starting materials for successive experiments. Run conditions and durations are listed in Table 1.

Unit-cell parameters were determined by least-squares refinement based on a triclinic unit-cell with space group $C\bar{1}$ and $Z = 1$. Chemical analyses were obtained with a JEOL electron microprobe (JXA 8600) applying operating conditions of 15 keV and 30 nA and the ZAF correction procedure. Details of the Mössbauer spectroscopic investigations can be found in Lougear *et al.* (2000) and are not repeated here. Heat capacity (C_p) was measured with a differential scanning calorimeter (Perkins Elmer DSC 7) at the Institute of Geoscience, Christian Albrechts University Kiel, in the temperature range 143–387 K. Experimental details were given by Bertoldi *et al.* (2001). The DSC measurements of 49 mg of powder in a closed pan in the temperature region 143–323 K were performed with heating rates of 20 K min^{-1} (two runs) and of 40 K min^{-1} (four runs) applying the step-scanning mode as described by Bosenick *et al.* (1996). The C_p data of the six DSC runs are listed in Table 2.

Low-temperature heat capacities of berthierine, corundum (standard reference material SRM-720, Dittmars *et al.*, 1982) and quartz were measured in the temperature range 5–300 K with the heat capacity option of the Physical Properties Measurement System (PPMS), produced by Quantum Design®. This device operates on the principles of heat-pulse calorimetry (HPC) and allows heat capacity measurements on milligram-sized samples (Dachs and Bertoldi, 2005). The HPC measurements were repeated three times at each temperature step (Table 3). The sample in the 1st series of measurements was a solid piece of run product, weighing 11.7 mg, measured directly on the sample platform. In the 2nd series, 12.4 mg of powdered sample were enclosed in an Al pan before the C_p measurement was performed. The C_p of the empty Al container was then subtracted from the total C_p to get C_p of the sample (see Dachs and Bertoldi, 2005, for further details). As shown by these authors, standard entropies of corundum (SRM-720), sanidine and fayalite were reproduced with a relative error of $\leqslant 0.5\%$ using single-crystal and sintered-powder samples, and were 1–2% too low for sealed powder-samples using a PPMS. The standard entropy $S_o = \int_0^{298.15} \frac{C_p}{T} dT$ of berthierine was calculated by splitting the measured low-T C_p-T data into three parts fitting each to a C_p polynomial of the form: $C_p = k_o + k_1 T^{-0.5} + k_2 T^{-2} + k_3 T^{-3}$ $(+ k_4 T + k_5 T^2 + k_6 T^3)$

Table 1. Run conditions of berthierine synthesis experiments.

	Starting material	Cumulative run duration (d)	T (ºC)	P (GPa)	Products
CHA#12/1	Glass	90	575	0.5	bert, qtz
CHA#12/2	CHA#12/1	96	575	0.5	bert, qtz
CHA#12/3	CHA#12/2	125	575	0.5	bert, qtz
CHA#12/4	CHA#12/3	154	575	0.5	bert, qtz
CHA#12/5	CHA#12/4	214	575	0.5	bert, qtz

bert: berthierine; qtz: quartz

https://doi.org/10.1346/CCMN.2005.0530406 Published online by Cambridge University Press

Table 2. Low-temperature heat capacities derived by DSC of berthierine and quartz with an overall mole weight of 397.136 g mol^{-1}. T in K; C_p in J/(mol K).

T	C_p	T	C_p	T	C_p	T	C_p	T	C_p	T	C_p	T	C_p
1st Series		307.2	265.2	269.2	289.8	245.2	269.9	221.2	251.9	197.2	228.0	191.2	221.7
163.2	181.2	309.2	267.2	271.2	290.9	247.2	271.3	223.2	253.9	199.2	230.6	193.2	225.0
165.2	183.7	311.2	269.2	273.2	292.2	249.2	273.0	225.2	260.1	201.2	233.4	195.2	228.1
167.2	186.0	313.2	271.2	275.2	293.5	251.2	274.8	227.2	262.6	203.2	236.1	197.2	231.0
169.2	188.5	315.2	273.2	277.2	294.9	253.2	276.6	229.2	264.7	205.2	238.7	199.2	233.4
171.2	190.6	317.2	275.2	279.2	296.3	255.2	278.4	231.2	266.8	207.2	241.0	201.2	235.5
173.2	192.8	319.2	277.2	281.2	297.7	257.2	280.2	233.2	269.0	209.2	242.7	203.2	237.4
175.2	194.8	321.2	279.2	283.2	299.0	259.2	281.9	235.2	270.8	211.2	244.3	205.2	239.3
177.2	197.1	323.2	281.2	285.2	300.8	261.2	283.7	237.2	272.8	213.2	246.2	207.2	241.1
179.2	199.3	303.2	283.2	287.2	302.8	263.2	285.4	239.2	274.6	215.2	248.0	209.2	243.3
181.2	201.8	305.2	285.2	289.2	304.5	265.2	287.2	241.2	276.6	217.2	250.0	211.2	245.5
183.2	204.4	307.2	287.2	291.2	306.0	267.2	288.9	243.2	273.2	219.2	252.1	213.2	247.5
185.2	207.1	309.2	289.2	293.2	307.5	269.2	290.6	245.2	274.7	221.2	253.4	215.2	249.2
187.2	209.8	311.2	291.2	295.2	308.7	271.2	292.4	247.2	276.2	223.2	254.8	217.2	250.8
189.2	212.6	313.2	293.2	297.2	310.0	273.2	294.1	249.2	277.7	243.2	274.7	219.2	252.5
191.2	215.5	315.2	295.2	299.2	311.2	275.2	295.8	251.2	279.2	245.2	276.7	221.2	255.1
193.2	217.9	2nd Series		301.2	312.6	277.2	297.5	253.2	280.7	247.2	278.4	223.2	257.6
195.2	220.o	163.2	184.8	303.2	314.1	279.2	299.1	255.2	282.1	249.2	280.0	243.2	278.0
197.2	222.1	165.2	187.1	305.2	315.4	281.2	300.4	257.2	283.6	251.2	281.0	245.2	278.9
199.2	224.2	167.2	189.3	307.2	316.7	283.2	301.7	259.2	285.1	253.2	282.0	247.2	279.5
201.2	226.3	169.2	191.6	309.2	318.1	285.2	303.1	261.2	286.5	255.2	283.2	249.2	280.4
203.2	228.4	171.2	193.8	311.2	319.5	287.2	304.4	263.2	287.7	257.2	284.5	251.2	281.3
205.2	230.5	173.2	196.0	313.2	320.7	289.2	305.7	265.2	289.1	259.2	285.5	253.2	282.7
207.2	232.6	175.2	198.3	315.2	321.9	291.2	307.0	267.2	290.3	261.2	286.5	255.2	283.4
209.2	234.6	177.2	200.5	317.2	323.1	293.2	308.3	269.2	291.9	263.2	287.9	257.2	285.0
211.2	236.7	179.2	202.7	319.2	324.2	295.2	309.6	271.2	293.6	265.2	289.4	259.2	287.0
213.2	238.8	181.2	204.9	321.2	325.4	297.2	310.9	273.2	295.0	267.2	290.8	261.2	289.0
215.2	240.8	183.2	207.1	323.2	326.3	299.2	312.1	275.2	296.3	269.2	292.2	263.2	291.0
217.2	242.8	185.2	209.2	3rd Series		301.2	313.4	277.2	297.7	271.2	293.7	265.2	292.9
219.2	244.8	187.2	211.4	163.2	186.8	303.2	314.6	279.2	299.1	273.2	295.8	267.2	294.7
221.2	246.8	189.2	213.6	165.2	189.0	305.2	315.9	281.2	300.8	275.2	298.3	269.2	296.5
223.2	248.7	191.2	215.7	167.2	190.9	307.2	317.1	283.2	302.5	277.2	300.9	271.2	298.0
225.2	250.6	193.2	218.4	169.2	193.0	309.2	318.3	285.2	304.1	279.2	303.1	273.2	300.0
227.2	252.5	195.2	220.8	171.2	195.1	311.2	319.6	287.2	305.8	281.2	305.1	275.2	301.6
229.2	254.4	197.2	222.9	173.2	197.4	313.2	321.4	289.2	307.4	283.2	306.9	277.2	303.4
231.2	256.3	199.2	224.9	175.2	199.4	315.2	323.3	291.2	309.0	285.2	308.6	279.2	305.0
233.2	258.2	201.2	226.9	177.2	201.6	317.2	325.1	293.2	310.6	287.2	309.5	281.2	306.7
235.2	260.1	203.2	229.0	179.2	203.8	319.2	326.9	295.2	312.3	289.2	310.1	283.2	308.1
237.2	262.0	205.2	231.0	181.2	206.2	321.2	328.5	297.2	313.9	291.2	310.6	285.2	308.9
239.2	263.8	207.2	233.0	183.2	208.3	323.2	330.1	299.2	315.4	293.2	311.4	287.2	310.0
241.2	265.7	209.2	235.0	185.2	210.4	4th Series		301.2	317.0	295.2	312.4	289.2	311.2
243.2	267.5	211.2	237.0	187.2	212.5	163.2	186.8	303.2	318.6	297.2	314.1	291.2	312.2
245.2	269.2	213.2	238.9	189.2	214.6	165.2	189.0	305.2	320.2	299.2	316.3	293.2	313.1
247.2	270.7	215.2	240.9	191.2	216.7	167.2	191.2	307.2	321.7	301.2	317.7	295.2	314.1
249.2	272.1	217.2	242.9	193.2	218.8	169.2	193.4	309.2	323.3	303.2	319.0	297.2	315.2
251.2	273.6	219.2	244.8	195.2	221.0	171.2	195.5	311.2	324.8	305.2	320.7	299.2	316.4
253.2	275.0	221.2	246.9	197.2	223.6	173.2	197.7	313.2	326.3	307.2	323.0	301.2	318.6
255.2	276.5	223.2	248.9	199.2	226.0	175.2	199.8	315.2	327.8	309.2	325.5	303.2	320.8
257.2	277.9	225.2	252.2	201.2	228.3	177.2	202.0	317.2	329.3	311.2	327.9	305.2	322.9
259.2	279.3	227.2	254.3	203.2	230.7	179.2	204.1	319.2	330.8	313.2	330.1	307.2	325.1
261.2	280.8	229.2	256.4	205.2	232.9	181.2	206.2	321.2	332.3	315.2	332.2	309.2	327.0
263.2	282.2	231.2	258.4	207.2	235.0	183.2	208.8	323.2	333.8	317.2	333.6	311.2	328.8
265.2	283.6	233.2	260.5	209.2	237.0	185.2	211.7	5th Series		319.2	335.3	313.2	330.4
267.2	284.9	235.2	262.2	211.2	238.6	187.2	214.8	163.2	186.9	321.2	337.0	315.2	332.5
269.2	286.3	237.2	264.1	213.2	240.5	189.2	217.4	165.2	189.7	323.2	338.5	317.2	334.9
271.2	287.7	239.2	265.9	215.2	242.5	191.2	220.0	167.2	192.1	6th Series		319.2	337.1
273.2	289.0	241.2	267.3	217.2	244.5	193.2	222.3	169.2	194.6	163.2	188.6	321.2	338.9
275.2	290.4	243.2	267.7	219.2	246.6	195.2	224.5	171.2	196.8	165.2	190.9	323.2	340.3
277.2	291.7	245.2	269.4	221.2	248.7	197.2	226.6	173.2	199.1	167.2	193.2		
279.2	293.1	247.2	271.2	223.2	250.5	199.2	228.8	175.2	201.0	169.2	195.5		
281.2	294.4	249.2	272.9	225.2	256.3	201.2	230.9	177.2	203.3	171.2	197.8		
283.2	295.7	251.2	274.4	227.2	257.6	203.2	233.1	179.2	205.4	173.2	200.0		
285.2	297.0	253.2	276.1	229.2	259.3	205.2	235.2	181.2	207.7	175.2	202.3		
287.2	298.3	255.2	277.8	231.2	261.3	207.2	237.3	183.2	210.0	177.2	204.6		
289.2	299.6	257.2	279.8	233.2	263.5	209.2	239.4	185.2	212.3	179.2	206.8		
291.2	300.9	259.2	281.7	235.2	265.7	211.2	241.5	187.2	214.9	181.2	209.1		
293.2	302.1	261.2	283.5	237.2	268.0	213.2	243.6	189.2	217.9	183.2	211.3		
295.2	303.4	263.2	285.4	239.2	270.3	215.2	245.7	191.2	220.1	185.2	213.5		
303.2	308.3	265.2	287.1	241.2	272.7	217.2	247.8	193.2	222.7	187.2	215.7		
305.2	263.2	267.2	288.5	243.2	268.5	219.2	249.8	195.2	225.4	189.2	218.2		

https://doi.org/10.1346/CCMN.2005.0530406 Published online by Cambridge University Press

Table 3. Low-temperature heat capacities derived by HPC of berthierine and quartz with an overall mole weight of 397.136 g mol^{-1}. T in K; C_p in J/(mol K).

T	C_p	1 σ	T	C_p	1 σ	T	C_p	1 σ	T	C_p	1 σ
1st Series			50.89	43.2	0.1	7.068	5.15	0.02	50.43	40.0	0.5
5.048	3.34	0.05	50.91	43.1	0.1	7.684	5.72	0.02	50.44	39.9	0.5
5.048	3.36	0.04	56.47	49.8	0.1	7.695	5.71	0.02	54.83	44.6	0.6
5.051	3.36	0.04	56.51	49.8	0.1	7.696	5.72	0.02	54.93	45.1	0.5
5.600	3.93	0.05	56.56	49.8	0.1	8.369	6.29	0.03	54.93	45.2	0.6
5.612	4.01	0.05	62.72	57.0	0.1	8.378	6.29	0.02	59.72	50.0	0.6
5.614	4.01	0.05	62.74	57.1	0.2	8.379	6.29	0.02	59.83	50.6	0.6
6.225	4.70	0.05	62.85	57.1	0.1	9.112	6.87	0.03	59.83	50.6	0.6
6.233	4.70	0.05	69.66	65.9	0.1	9.122	6.84	0.02	65.05	56.4	0.6
6.235	4.71	0.05	69.67	65.9	0.2	9.123	6.88	0.02	65.17	57.1	0.7
6.910	5.43	0.05	69.84	66.0	0.1	9.923	7.45	0.03	65.17	57.2	0.7
6.933	5.49	0.04	77.37	75.4	0.2	9.933	7.45	0.02	70.85	63.7	0.7
6.935	5.48	0.07	77.38	75.1	0.2	9.934	7.44	0.02	70.97	64.2	0.7
7.679	6.19	0.05	77.59	75.5	0.2	10.82	8.02	0.03	70.98	64.0	0.7
7.685	6.19	0.05	85.92	86.1	0.2	10.83	8.02	0.02	77.15	72.1	0.7
7.687	6.19	0.05	85.94	86.1	0.2	10.83	8.02	0.02	77.29	72.5	0.8
8.530	6.96	0.05	86.21	86.2	0.2	11.80	8.59	0.03	77.29	72.4	0.8
8.537	6.97	0.05	95.36	98.2	0.3	11.81	8.60	0.02	84.06	81.0	0.7
8.538	6.97	0.05	95.44	98.3	0.2	11.81	8.60	0.02	84.19	82.1	0.8
9.474	7.71	0.05	95.47	98.3	0.2	12.84	9.20	0.04	84.20	82.1	0.9
9.481	7.71	0.05	105.8	113.1	0.3	12.85	9.21	0.02	91.55	91.9	0.8
9.482	7.71	0.05	106.0	113.2	0.2	12.85	9.21	0.02	91.69	92.6	0.8
10.53	8.46	0.05	106.0	113.2	0.2	13.98	9.85	0.04	91.69	92.7	0.9
10.53	8.45	0.05	117.6	130.8	0.3	13.99	9.85	0.03	99.68	102.6	0.9
10.53	8.44	0.05	117.7	131.0	0.3	13.99	9.85	0.03	99.83	103.6	0.9
11.69	9.20	0.05	117.7	131.0	0.3	15.22	10.56	0.04	99.83	103.5	1.0
11.70	9.20	0.05	130.6	148.3	0.3	15.24	10.56	0.03	108.6	115.5	1.0
11.70	9.20	0.05	130.8	148.5	0.3	15.24	10.56	0.03	108.8	115.6	0.9
12.99	10.05	0.05	130.8	148.4	0.3	16.57	11.34	0.05	108.8	116.2	1.0
12.99	10.04	0.05	145.0	167.5	0.3	16.59	11.36	0.03	118.3	128.8	1.0
13.00	10.04	0.05	145.2	167.6	0.4	16.59	11.36	0.03	118.4	128.9	0.8
14.43	10.94	0.05	145.2	167.7	0.3	18.05	12.24	0.05	118.4	129.0	1.0
14.43	10.94	0.04	161.1	186.5	0.4	18.07	12.27	0.04	128.8	142.9	1.0
14.43	10.94	0.04	161.2	186.7	0.4	18.07	12.27	0.04	129.0	143.1	0.9
16.02	11.95	0.05	161.2	186.7	0.4	19.66	13.26	0.05	129.0	143.7	1.0
16.03	11.95	0.04	178.9	207.1	0.4	19.68	13.30	0.04	140.3	158.2	1.0
16.03	11.95	0.04	179.0	207.4	0.5	19.68	13.29	0.05	140.5	158.2	0.9
17.79	13.11	0.05	179.1	207.2	0.4	21.39	14.38	0.07	140.5	158.8	1.1
17.80	13.11	0.04	198.8	228.0	0.5	21.41	14.44	0.06	152.8	173.7	1.1
17.81	13.12	0.04	198.8	228.1	0.5	21.42	14.44	0.06	153.0	173.9	1.0
19.76	14.48	0.05	198.9	228.2	0.5	23.30	15.72	0.06	153.0	173.9	1.2
19.77	14.49	0.04	220.8	249.9	0.5	23.33	15.77	0.07	166.5	190.1	1.2
19.78	14.49	0.04	220.9	249.7	0.6	23.33	15.78	0.07	166.7	190.1	0.9
21.94	16.06	0.05	220.9	249.6	0.6	25.37	17.24	0.11	166.7	190.3	1.2
21.96	16.09	0.04	245.3	273.7	0.6	25.41	17.31	0.09	181.3	207.7	1.5
21.96	16.09	0.04	245.3	273.6	0.7	25.41	17.30	0.09	181.5	206.0	1.0
24.37	17.93	0.05	245.4	273.9	0.7	27.64	19.0	0.1	181.5	206.7	1.2
24.39	17.97	0.05	272.4	294.5	0.7	27.68	19.1	0.1	197.6	225.5	1.6
24.39	17.95	0.05	272.4	294.6	0.7	27.68	19.1	0.1	197.8	224.0	1.0
27.07	20.13	0.06	272.4	298.6	0.7	30.11	21.0	0.2	197.8	224.5	1.3
27.09	20.16	0.05	302.4	314.1	0.8	30.16	21.1	0.1	215.3	244.3	1.6
27.09	20.17	0.05	302.4	314.1	0.8	30.16	21.1	0.1	215.5	243.0	1.1
30.07	22.67	0.06	302.6	314.7	0.8	32.80	23.1	0.2	215.5	243.0	1.4
30.09	22.70	0.05	2nd series			32.86	23.3	0.2	234.5	269.2	1.7
30.10	22.71	0.05	5.002	3.06	0.02	32.86	23.4	0.2	234.6	265.0	1.1
33.41	25.65	0.08	5.009	3.07	0.02	35.74	25.6	0.3	234.7	267.4	1.4
33.43	25.70	0.06	5.019	3.09	0.01	35.81	25.9	0.2	255.4	287.0	1.6
33.44	25.70	0.06	5.461	3.54	0.02	35.81	25.9	0.2	255.6	286.8	1.1
37.12	29.07	0.08	5.465	3.54	0.02	38.95	28.5	0.3	255.6	288.5	1.5
37.13	29.12	0.07	5.467	3.54	0.02	39.02	28.8	0.3	278.2	303.4	1.6
37.15	29.13	0.07	5.948	4.05	0.02	39.02	28.8	0.3	278.2	302.8	1.1
41.24	33.02	0.08	5.955	4.06	0.02	42.42	31.6	0.3	278.3	303.5	1.6
41.25	32.99	0.08	5.956	4.05	0.02	42.51	32.0	0.3	303.1	317.6	1.1
41.26	33.05	0.09	6.476	4.59	0.02	42.51	32.0	0.4	303.1	319.3	1.7
45.79	37.74	0.09	6.482	4.58	0.02	46.21	35.3	0.4	303.1	319.5	1.4
45.82	37.73	0.09	6.499	4.53	0.11	46.30	35.8	0.4			
45.83	37.8	0.1	7.066	5.15	0.02	46.31	35.7	0.4			
50.86	43.1	0.1	7.066	5.19	0.02	50.33	39.4	0.5			

https://doi.org/10.1346/CCMN.2005.0530406 Published online by Cambridge University Press

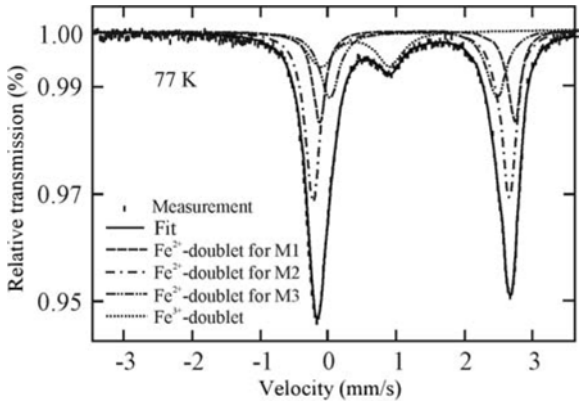

Figure 1. Mössbauer spectrum of berthierine (CHA#12/4) taken at 77 K in zero field simulated with the Mössbauer parameters of Table 2.

using the Experimental Data Analyst package of Mathematica®. This procedure guaranteed best reproduction of the experimental data and the integral was then analytically solved for the boundaries of these intervals. The C_p values below 5 K were estimated by a linear extrapolation to 0 K in a plot of C_p/T *vs.* T^2 and contribute to the standard entropy with 1.02 J mol^{-1} K^{-1}.

The uncertainty of the standard entropy S_o was estimated by applying a Monte Carlo technique to the measured PPMS C_p data and their standard deviations using the Mathematica functions RandomArray and NormalDistribution to calculate a randomly distributed error for each measurement. Thus a set of synthetic C_p data was created and integrated to get S_o. This procedure was repeated 1000 times and the mean and standard deviation of these data gave S_o and σ_{S_o}. Note that, because errors tend to cancel out in the integration, the relative uncertainty σ_{S_o}/S_o is smaller than σ_{Cp}/C_p.

An additional synthesis experiment was carried out in a piston-cylinder apparatus with a 125 mm diameter pressure chamber at the University of Stuttgart (run CHA#S). The experimental charge was enclosed in an inner $Ag_{70}Pd_{30}$ capsule (7 by 4 mm) and the experiment

Table 4. Mössbauer parameters of the measured berthierine (CHA#12/4) at 77 K in zero field; δ: isomer shift; ΔE_Q: quadrupole splitting; Γ: full width at half maximum; A: area.

Doublet	δ (mm s^{-1})	ΔE_Q (mm s^{-1})	Γ (mm s^{-1})	A (%)
Fe^{2+} M1	1.27	2.43	0.34	20
Fe^{2+} M2	1.22	2.85	0.26	43
Fe^{2+} M3	1.32	2.84	0.23	22
Fe^{3+}	0.43	1.01	0.47	15

was run at 2.3 GPa, 475ºC for 5 days. The starting material was an oxidized, brownish gel of the composition $2.3Fe_2O_3{\cdot}1.4Al_2O_3{\cdot}2.6SiO_2$. The oxygen fugacity during the experiment was controlled as suggested by Eugster and Wones (1962) using an Fe/FeO mixture plus water sealed in an outer capsule made of Fe (11 by 6 mm). After the experiment, the color of the experimental charge changed to light green, indicating the efficiency of the buffer.

The HRTEM investigations were performed at the Forschungsinstitut für Elektronenmikroskopie und Feinstrukturforschung, University of Technology, Graz, and at the GeoForschungsZentrum, Potsdam (Section 4.1: Experimental Geochemistry and Mineral Physics) in order to ensure that the synthesis products used for calorimetry (CHA#12/4 and CHA#S) were indeed berthierine structurally.

RESULTS AND DISCUSSION

As proven by XRD, berthierine and quartz were the products in all hydrothermal runs (Table 1). The transformation of berthierine to chamosite was never demonstrated in our experiments, in spite of cumulative run times of up to 214 days, exceeding by far the predicted run duration of 60 days for a complete transformation according to James *et al.* (1976). The successful synthesis of the 2:1 mineral chamosite in the piston-cylinder run demonstrates that the transformation

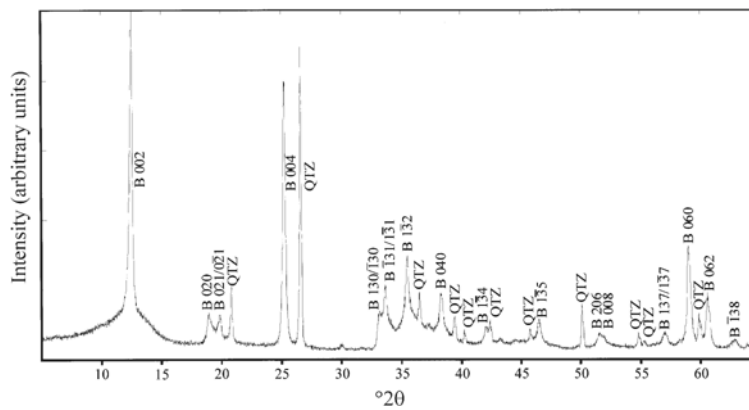

Figure 2. XRD (º2θ CuKα) pattern of the run product Cha12#4 (B: berthierine, QTZ: quartz). For further discussion see text.

https://doi.org/10.1346/CCMN.2005.0530406 Published online by Cambridge University Press

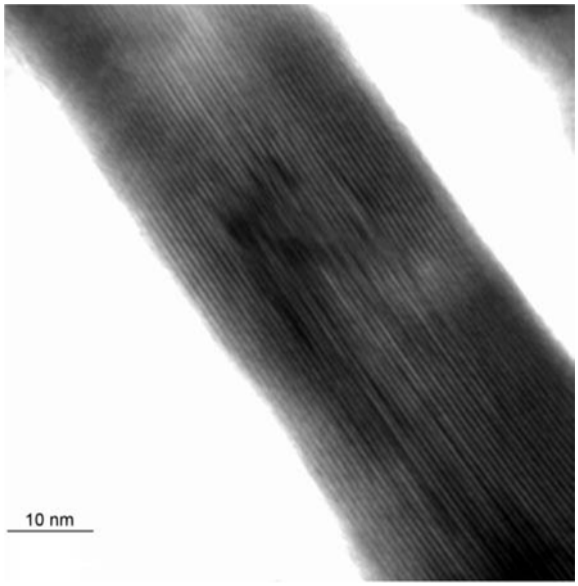

Figure 3. TEM image of the hydrothermal run product Cha12#4 showing half zipper-like strips which correspond to 1:1 layers of berthierine.

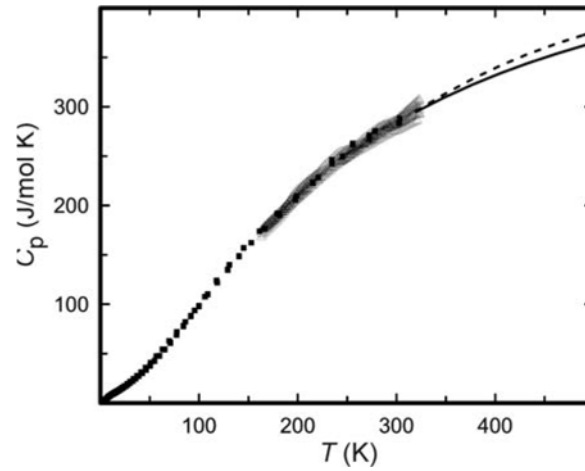

Figure 5. Heat capacities of berthierine corrected for the end-member composition $(Fe_{2.5}Al_{0.5})[Si_{1.5}Al_{0.5}O_5](OH)_4$ (squares PPMS, triangles DSC) and extrapolation to higher temperatures using the model adopted by this study (solid line, based on Berman and Brown, 1985), and the Debye model (broken line).

of berthierine to chamosite depends mainly on pressure under experimental conditions.

The Mössbauer spectrum of berthierine (CHA#12/4) was analyzed with three Lorentzian-shaped doublets for Fe^{2+} and one doublet for Fe^{3+} (Figure 1 and Table 4). The ratio $Fe^{3+}/\Sigma Fe$ is 0.15.

The calculated formula derived by electron microprobe analyses and Mössbauer spectroscopy of run CHA#12/4, on the basis of 7 oxygens, is: $(Fe^{2+}_{1.83}Fe^{3+}_{0.33}Al)[Si_{1.33}Al_{0.67}O_5(OH)_4$. The calculated unit-cell parameters are: a_o = 5.388(3) Å, b_o = 9.377(2) Å, c_o = 7.040(3) Å, α = 89.96(2)°, β = 90.06(2)°, γ = 90.16(5)° and V = 107.098 cm^3 mol^{-1}. The XRD pattern reveals that the periodicity along [001] is 7 Å (*e.g.* absence of reflections at ~6.2° and 31.6°2θ, which should appear as the 001 and 005 reflections of chlorite, respectively, as seen in Figure 2. This is further confirmed by the HRTEM investigation of run CHA#12/4, which shows half zipper-like strips of trioctahedral 1:1 layers of berthierine (Figure 3). On

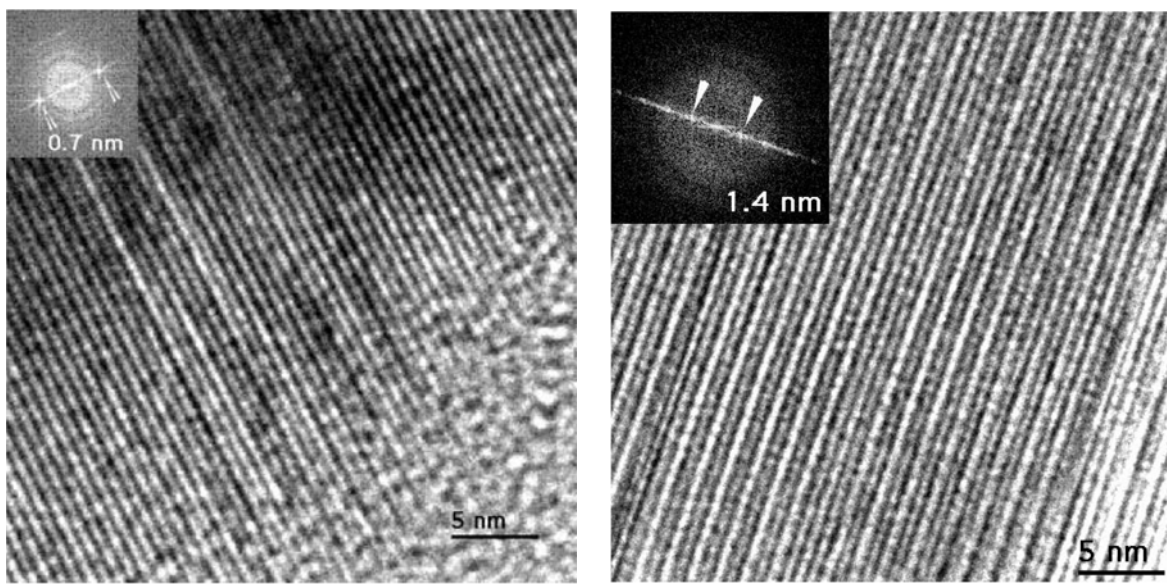

Figure 4. Energy filtered lattice-fringe images of the piston-cylinder run product CHA#S showing typical half zipper-like strips which correspond to 1:1 layers of berthierine with a basal spacing (001) of 0.7 nm (left) and typical zipper-like strips which correspond to 2:1 layers of chamosite with a basal spacing (001) of 1.4 nm (right). The corresponding diffraction patterns show the 001 reflections with reciprocal spacings corresponding to 0.7 nm and 1.4 nm, respectively.

https://doi.org/10.1346/CCMN.2005.0530406 Published online by Cambridge University Press

Table 5. Heat capacities of quartz, corundum: HPC – measurements performed by this study (temperatures given are mean values of the three repeated PPMS measurements); heat capacities at temperatures of the DSC measurements were calculated with the model of Berman and Brown (1985). C_p of wüstite is according to Stølen *et al.* (1996). These data were used for the corrections to end-member berthierine $(Fe_{2.5}Al_{0.5})[Si_{1.5}Al_{0.5}O_5](OH)_4$. T in K; C_p J/(mol K).

HPC T	Quartz C_p	Corundum C_p	Wüstite C_p	HPC T	Quartz C_p	Corundum C_p	Wüstite C_p	DSC T	Quartz C_p	Corundum C_p	Wüstite C_p
1st Series				30.15	2.177	0.281	1.687	227.2	35.89	60.90	43.87
5.049	0.005	0.002	0.011	32.84	2.648	0.370	2.130	229.2	36.14	61.52	44.00
5.609	0.007	0.002	0.014	35.78	3.165	0.489	2.684	231.2	36.39	62.13	44.14
6.231	0.009	0.003	0.019	39.00	3.754	0.651	3.373	233.2	36.64	62.74	44.26
6.926	0.013	0.004	0.025	42.48	4.411	0.866	4.217	235.2	36.89	63.34	44.39
7.684	0.018	0.006	0.033	46.27	5.130	1.155	5.239	237.2	37.14	63.93	44.51
8.535	0.026	0.008	0.044	50.40	5.917	1.543	6.457	239.2	37.38	64.52	44.65
9.479	0.039	0.010	0.059	54.90	6.781	2.062	7.887	241.2	37.63	65.10	44.81
10.53	0.059	0.014	0.080	59.79	7.725	2.756	9.538	243.2	37.87	65.67	44.96
11.70	0.090	0.019	0.108	65.13	8.757	3.635	11.41	245.2	38.11	66.24	45.10
12.99	0.138	0.025	0.146	70.94	9.873	4.763	13.50	247.2	38.23	66.52	45.24
14.43	0.209	0.033	0.198	77.24	11.06	6.207	15.78	248.2	38.35	66.80	45.31
16.03	0.313	0.044	0.148	84.15	12.33	8.018	18.24	249.2	38.59	67.36	45.38
17.80	0.457	0.059	0.211	91.64	13.63	10.21	20.85	251.2	38.82	67.91	45.51
19.77	0.654	0.079	0.392	99.78	15.10	12.83	23.52	253.2	39.06	68.45	45.64
21.95	0.913	0.107	0.631	108.7	17.03	15.92	26.10	255.2	39.29	68.99	45.76
24.38	1.246	0.146	0.912	118.4	18.90	19.48	28.58	257.2	39.40	69.26	45.88
27.08	1.662	0.201	1.251	129.0	20.81	23.59	31.00	258.2	39.52	69.53	45.94
30.09	2.167	0.280	1.678	140.5	22.79	28.17	33.31	259.2	39.75	70.06	46.00
33.42	2.751	0.392	2.234	152.9	24.84	33.05	35.51	261.2	39.97	70.58	46.11
37.13	3.399	0.553	2.963	166.6	27.02	38.46	37.62	263.2	40.20	71.10	46.22
41.25	4.179	0.785	3.908	181.4	29.28	44.25	39.57	265.2	40.42	71.61	46.33
45.81	5.042	1.116	5.110	197.7	31.65	50.34	41.38	267.2	40.54	71.87	46.44
50.88	6.009	1.593	6.606	215.4	34.09	56.49	42.99	268.2	40.65	72.12	46.49
56.51	7.091	2.275	8.422	234.6	36.58	62.57	44.35	269.2	40.87	72.62	46.54
62.77	8.301	3.239	10.58	255.6	39.11	68.58	45.78	271.2	41.09	73.12	46.64
69.72	9.639	4.509	13.06	278.2	41.64	74.35	46.98	273.2	41.31	73.61	46.74
77.45	11.10	6.259	15.86	303.1	45.26	80.10	47.99	275.2	41.52	74.10	46.84
86.02	12.66	8.545	18.89					277.2	41.63	74.34	46.93
95.42	14.24	11.40	22.13	DSC	Quartz	Corundum	Wüstite	278.2	41.74	74.58	46.98
106.0	16.47	14.95	25.34	T	C_p	C_p	C_p	279.2	41.95	75.06	47.02
117.7	18.77	19.23	28.42	163.2	26.79	37.88	37.11	281.2	42.16	75.53	47.11
130.7	21.11	24.26	31.36	165.2	27.10	38.67	37.40	283.2	42.37	76.00	47.20
145.1	23.56	30.02	34.17	167.2	27.41	39.46	37.69	285.2	42.58	76.47	47.29
161.2	26.17	36.31	36.82	169.2	27.72	40.25	37.97	287.2	42.69	76.70	47.37
179.0	28.92	43.33	39.27	171.2	28.03	41.04	38.25	288.2	42.79	76.93	47.41
198.8	31.81	50.74	41.49	173.2	28.34	41.83	38.52	289.2	43.00	77.38	47.45
220.9	34.82	58.29	43.41	175.2	28.64	42.61	38.78	291.2	43.20	77.83	47.53
245.3	37.89	65.71	45.11	177.2	28.94	43.38	39.04	293.2	26.79	37.88	47.61
272.4	41.01	72.93	46.70	179.2	29.24	44.16	39.29	295.2	43.40	78.28	47.69
302.5	45.20	79.97	47.97	181.2	29.54	44.92	39.54	297.2	43.61	78.72	47.77
2nd Series				183.2	29.84	45.69	39.78	301.2	45.06	79.68	47.92
5.009	0.005	0.002	0.011	185.2	30.13	46.44	40.02	303.2	45.26	80.11	47.99
5.464	0.006	0.002	0.013	187.2	30.42	47.19	40.25	305.2	45.47	80.53	48.06
5.953	0.008	0.003	0.017	189.2	30.71	47.94	40.47	307.2	45.67	80.94	48.13
6.486	0.011	0.004	0.021	191.2	31.00	48.68	40.69	308.2	45.77	81.14	48.17
7.066	0.014	0.005	0.026	193.2	31.29	49.41	40.91	309.2	45.87	81.35	48.20
7.692	0.018	0.006	0.033	195.2	31.57	50.14	41.12	311.2	46.07	81.75	48.27
8.375	0.025	0.007	0.042	197.2	31.86	50.86	41.32	313.2	46.27	82.15	48.33
9.119	0.034	0.009	0.053	199.2	32.14	51.58	41.52	315.2	46.47	82.55	48.40
9.93	0.046	0.012	0.067	201.2	32.42	52.29	41.72	317.2	46.67	82.94	48.47
10.83	0.066	0.015	0.086	203.2	32.70	52.99	41.91	318.2	46.77	83.13	48.50
11.80	0.093	0.019	0.110	205.2	32.97	53.69	42.10	319.2	46.86	83.32	48.53
12.85	0.132	0.024	0.141	207.2	33.25	54.37	42.28	321.2	47.06	83.71	48.59
13.99	0.185	0.03	0.181	209.2	33.52	55.06	42.46	323.2	47.25	84.08	48.65
15.23	0.258	0.038	0.194	211.2	33.79	55.73	42.63	321.2	47.06	83.71	48.59
16.59	0.355	0.049	0.149	213.2	34.06	56.40	42.80	323.2	47.25	84.08	48.65
18.06	0.481	0.062	0.231	215.2	34.32	57.06	42.97				
19.67	0.643	0.078	0.382	217.2	34.59	57.72	43.13				
21.41	0.845	0.100	0.569	219.2	34.85	58.37	43.28				
23.32	1.096	0.128	0.787	221.2	35.11	59.01	43.44				
25.40	1.398	0.165	1.036	223.2	35.37	59.65	43.58				
27.67	1.758	0.215	1.330	225.2	35.63	60.28	43.73				

https://doi.org/10.1346/CCMN.2005.0530406 Published online by Cambridge University Press

the other hand, the HRTEM investigation of the piston cylinder run CHA#S shows periodicities along the *c* axis of both 14 and 7 Å (SAED patterns in Figure 4). About two thirds of the run product consist of chamosite.

From the mineral-chemical analyses the following synthesis reaction can be deduced:

$$0.720\ Fe_3Al_2Si_3O_{12}(gel) + 2.000\ H_2O(v) + 0.085\ O_2(v) \rightleftharpoons (Fe^{2+}_{1.83}Fe^{3+}_{0.33}Al)[Si_{1.33}Al_{0.67}O_5](OH)_4(s) + 0.830\ SiO_2(s) + 0.055\ Al_2O_3(s) \quad (1)$$

We recognize from this reaction that a mixture of berthierine and quartz with an overall mole weight of 397.136 g mol^{-1} has formed in the synthesis experiments. A small amount of an Al_2SiO_5 phase could have formed according to equation 1, but was not detected by XRD. The results of our C_p measurements are listed in Tables 2 (DSC data) and 3 (PPMS-data). The agreement between C_p data of the 1st and 2nd series, as measured by HPC, is satisfactory. At temperatures <220 K, the C_p data of the 1st series (obtained on an 11.7 mg solid piece of berthierine) are somewhat higher than those measured on the 12.4 mg powder sample and become somewhat lower at higher temperatures. The relative uncertainty of the data ($100\sigma_{C_p}/C_p$) is ~1% at low *T*, decreasing to 0.2–0.4% at higher temperatures.

The DSC data have a considerably larger error than the HPC data and the latter all lie within the error limit of the DSC data. The DSC measurements in the temperature range 373–423 K show that berthierine starts to decompose at ~370 K and ambient pressure. The HPC and DSC data at each temperature were corrected for 0.830 moles of quartz and 0.055 moles of corundum to yield the heat capacities of berthierine with the chemical composition given in equation 1. These C_p data were corrected to the end-member composition of berthierine $(Fe_{2.5}Al_{0.5})[Si_{1.5}Al_{0.5}O_5](OH)_4$ on the basis of the Neumann-Kopp rule using measured C_p values of quartz and corundum and the C_p of wüstite according to Stølen *et al.* (1996) (Table 5). The C_p data calculated thus of end-member berthierine are plotted in Figure 5.

The standard entropy, calculated via the relation $S_o = \int_0^{298.15} \frac{C_p}{T} dT$, is 284.1±0.3 J mol^{-1} K^{-1} for end-member berthierine. The estimated uncertainty is 0.35% of S_o, and is similar to the mean of relative uncertainties of C_p measurements from the 1st series. This calorimetrically derived value for S_o is in good agreement with 287.9±2.8 J $mol^{-1}K^{-1}$ derived according to the estimation method of Holland (1989) which is based on the dependence of entropy on volume. If the C_p of berthierine is estimated by combining the C_p polynomials for SiO_2, Al_2O_3, FeO and structural H_2O as given by Berman and Brown (1985, their Table 4), these C_p values are slightly higher at 298–323 K than the calorimetric data in that temperature range. Applying a factor of 0.99 to the calculated C_p data yields a good agreement between both sets and we use these data as an extrapolation of our calorimetrically determined C_p data to higher temperatures (Figure 5). A fit to this combined data set results in the C_p polynomial: $C_p = 610.72 - 5140.0T^{-0.5} - 5.8848 \times 10^6\ T^{-2} + 9.5444 \times 10^8\ T^{-3}$. At 3000 K, this polynomial yields 28.7 J/(a.p.f.u. K) (a.p.f.u. = atoms per formula unit), well within 28.3±2.0 J/(a.p.f.u. K) derived by Berman and Brown (1985) as a mean value of C_p of 91 minerals at this temperature. Alternatively, we used the Debye model to extrapolate C_p values to higher temperatures with a Debye temperature of 960 K. With this value, a good overlap of measured and calculated C_p values at the high-temperature end of the calorimetric data is obtained (298–325 K). At 3000 K, however, C_p per formula unit according to the Debye model is only 23.3 J/(a.p.f.u. K), demonstrating that this extrapolation yields values which are too low and we thus recommend the above given C_p polynomial for thermodynamic calculation involving berthierine above 298 K.

CONCLUSIONS

Heat capacities of well characterized synthetic berthierine have been measured in this study from 5 to 323 K using a PPMS and DSC. From these data we derived the standard entropy S_o and a C_p polynomial for end-member berthierine and thus we contribute to the knowledge on the thermodynamic properties of this phase. We recommend our data for use in thermodynamic calculations.

ACKNOWLEDGMENTS

This work was supported by the Fonds zur Förderung der wissenschaftlichen Forschung, Austria, project P15880-NO3, which is gratefully acknowledged. Thanks to Andre Lougear for performing the Mössbauer spectrum. Reviews by Alexandra Navrotsky, Giovanna Giorgetti and Peter Heaney helped to improve this manuscript.

REFERENCES

Aagaard, P., Jahren, J.S., Harstad, A.O., Nilsen, O. and Ramm, M. (2000) Formation of grain-coating chlorite in sandstones; laboratory synthesized *vs.* natural occurrences. *Clay Minerals*, **35**, 261–269.

Ahn, J.H. and Peacor, D.R. (1985) Transmission electron microscopic study of diagenetic chlorite in Gulf Coast argillaceous sediments. *Clays and Clay Minerals*, **33**, 328–336.

Bailey, S.W. (1980) Summary of recommendations of the AIPEA nomenclature committee. *The Canadian Mineralogist*, **18**, 143–150.

Bailey, S.W. (1988a) Structures and compositions of other trioctahedral 1:1 phyllosilicates. Pp. 169–188 in: *Hydrous Phyllosilicates (Exclusive of Micas)* (S.W. Bailey, editor) Reviews in Mineralogy, **19**. Mineralogical Society of America, Washington, D.C.

Bailey, S.W. (1988b) Odinite, a new dioctahedral-trioctahedral Fe^{3+}-rich 1:1 clay mineral. *Clay Minerals*, **23**, 237–247.

Berman, R.G. and Brown, T.H. (1985) Heat capacity of minerals in the system Na_2O-K_2O-CaO-MgO-FeO-Fe_2O_3-Al_2O_3-SiO_2-TiO_2-H_2O-CO_2: representation, estimation, and

high temperature extrapolation. *Contributions to Mineralogy and Petrology*, **89**, 168–183.

Bertoldi, C., Benisek, A., Cemič, L. and Dachs, E. (2001) The heat capacity of two natural chlorite group minerals derived from differential scanning calorimetry. *Physics and Chemistry of Minerals*, **28**, 332–336.

Bosenick, A., Geiger, Ch.A. and Cemic, L. (1996) Heat capacity measurements of synthetic pyrope-grossular between 320 and 1000 K by differential scanning calorimetry. *Geochimica et Cosmochimica Acta*, **60**, 3215–3227.

Cho, M. and Fawcett, J.J. (1986) A kinetic study of clinochlore and its high temperature assemblage, forsterite-cordierite-spinel at 2 kbar water pressure. *American Mineralogist*, **71**, 68–77.

Dachs, E. (1994) Annite stability revised. 1. Hydrogen-sensor data for the reaction Annite = sanidine + magnetite + H_2. *Contributions to Mineralogy and Petrology*, **117**, 229–240.

Dachs, E. and Bertoldi, C. (2005) Precision and accuracy of the heat-pulse calorimetric technique: Low-temperature heat capacities of milligram-sized synthetic mineral samples. *European Journal of Mineralogy*, in press.

Deer, W.A., Howie, R.A. and Zussman, J. (1992) *An Introduction to the Rock-forming Minerals*. Longman Scientific and Technical, New York.

Dittmars, D.A., Ishihara, S., Chang, S.S., Bernstein, G. and West, E.D. (1982) Measurement of the relative enthalpy of pure α-Al_2O_3 (NBS heat capacity and enthalpy standard reference material no. 720) from 10 to 1,950 K. *Journal of Research of the Natural Bureau of Standards*, **87**, 5–9.

Ehrenberg, S.N. (1993) Preservation of anomalously high porosity in deeply buried sandstones by grain-coating chlorite: examples Norwegian Continental Shelf. *American Association of Petroleum Geologists Bulletin*, **77**, 1260–1286.

Eugster, H.P. and Wones, D.R. (1962) Stability relations of the ferruginous biotite, annite. *Journal of Petrology*, **3**, 82–125

Gillery, F.H. (1959) X-ray study of synthetic Mg-Al serpentines and chlorites. *American Mineralogist*, **44**, 143–152.

Guggenheim, S., Alietti, A., Drits, V.A., Formoso, M.L.L., Galán, E., Köster, H.M., Paquet, H., Watanabe T. and ex officio members Bain, D.C. (Editor, *Clay Minerals*) and Hudnall, W.H. (Editor, *Clays and Clay Minerals*) (1997) Report of the Association Internationale Pour L'Étude des Argiles (AIPEA) Nomenclature Committee for 1996. *Clays and Clay Minerals*, **45**, 298–300.

Hillier, S. (1994) Pore-lining chlorites in siliclastic reservoir sandstones: electron microprobe, SEM, and XRD data, and implications for their origin. *Clay Minerals*, **29**, 665–679.

Holland, T.J.B. (1989) Dependence of entropy on volume for silicate and oxide minerals: A review and a predictive model. *American Mineralogist*, **74**, 5–13.

Holland, T.J.B. and Powell, R. (1998) An internally consistent thermodynamic data set for phases of petrological interest. *Journal of Metamorphic Geology*, **16**, 309–343.

Hornibrook, E.R.C. and Longstaffe, F.J. (1996) Berthierine from the lower Cretaceous Clearwater Formation, Alberta, Canada. *Clays and Clay Minerals*, **44**, 1–21.

Hsu, L.C. (1968) Selected phase relationships in the system Al-Mn-Fe-Si-O-H: A model for garnet equilibria. *Journal of Petrology*, **9**, 40–83.

Iijima, A. and Matsumoto, R. (1982) Berthierine and chamosite in coal measures of Japan. *Clays and Clay Minerals*, **30**, 264–274.

James, R.S., Turnock, A.C. and Fawcett, J.J. (1976) The stability and phase relations of iron chlorite below 8.5 kb P_{H_2O}. *Contributions to Mineralogy and Petrology*, **56**, 1–25.

Kisch, H.J. (1983) Mineralogy and petrology of burial diagenesis (burial metamorphism) and incipient metamorphism in clastic rocks. Pp. 289–493 in: *Diagenesis in Sediments and Sedimentary Rocks vol. 2* (F. Larsen and G.V. Chilingar, editors). Elsvier, New York.

López-Munguira, A. and Nieto, F. (2000) Transmission electron microscopy study of very-low grade metamorphic rocks in Cambrian sandstones and shales, Ossa-Morena zone, Southwest Spain. *Clays and Clay Minerals*, **48**, 213–223.

Lougear, A., Grodzicki, M., Bertoldi, C., Trautwein, X., Steiner, K. and Amthauer, G. (2000) Mössbauer and molecular orbital study of chlorites. *Physics and Chemistry of Minerals*, **27**, 258–269.

Mata, V., Giorgetti G., Arkai P. and Peacor D.R. (2001) Comparison of evolution of triooctahedral chlorite/berthierine/smectite in coeval metabsites and metapelites from diagenetic to epizonal grades. *Clays and Clay Minerals*, **49**, 318–332.

Nelson, B.W. and Roy, R. (1958) Synthesis and stability of minerals in the system MgO-Al_2O_3-SiO_2-H_2O. *American Mineralogist*, **40**, 147–178.

Odin, G.S. (1990) Clay mineral formation at the continent-ocean boundary: the verdine facies. *Clay Minerals*, **25**, 477–483.

Odin, G.S. and Sen Gupta, B.K. (1988) Geological significance of the verdine facies. Pp. 205–219 in: *Green Marine Clays* (G.S. Odin, editor). Developments in Sedimentology, **45**, Elsevier, Amsterdam.

Odin, G.S., Bailey, S.W., Amourice, M., Frohlich, F. and Waychunas, G.S. (1988) Mineralogy of the verdine facies. Pp. 159–206 in: *Green Marine Clays* (G.S. Odin, editor). Developments in Sedimentology, **45**, Elsevier, Amsterdam.

Porrenga, D.H. (1967) Glauconite and chamosite as depth indicators in the marine environments. *Marine Geology*, **5**, 495–501.

Ryan, P.C. and Hillier S. (2002) Berthierine/chamosite, corrensite and discrete chlorite from evolved verdine and evaporite facies in the Jurassic Sundance Formation, Wyoming. *American Mineralogist*, **87**, 1607–1615.

Ryan, P.C. and Reynolds, R.C. (1996) The origin and diagenesis of grain-coating serpentine-chlorite in Tuscaloosa Formation sandstone, U.S. Gulf Coast. *American Mineralogist*, **81**, 213–225.

Schmidt, D., Livi, K.J.T., and Frey, M. (1999) Reaction progress in chloritic minerals: An electron microbeam study of the Taveyanne greywacke, Switzerland. *Journal of Metamorphic Geology*, **17**, 229–241.

Stølen, S., Glöckner, R., Grønvold, F., Atake, T. and Izumisawa, S. (1996) Heat capacity and nearly stoichiometric wüstite from 13 to 450 K. *American Mineralogist*, **81**, 973–981.

Toth, T.A. and Fritz, S.J. (1997) An Fe-berthierine from a cretaceous laterite: Part I. Characterization. *Clays and Clay Minerals*, **45**, 564–579.

Turnock, A.C. (1960) The stability of iron chlorites. *Carnegie Institute of Washington Yearbook*, **59**, 98–103.

Velde, B. (1985) *Clay Minerals: a Physico-Chemical Explanation of their Occurrence.* Elsvier, Amsterdam and New York.

Walker, J.R. and Thompson, G.R. (1990) Structural variations in chlorite and illite in a diagenetic sequence from the Imperial Valley. California. *Clays and Clay Minerals*, **38**, 315–321.

Yoder, H.S., Jr. (1952) The MgO-Al_2O_3-SiO_2-H_2O system and the related metamorphic facies. *American Journal of Science*, **250-A**, 569–627.

(*Received 14 December 2004; revised 14 March 2005; Ms. 990; A.E. Peter J. Heaney*)